Reaction $\pi^+ + d \rightarrow p + p$ at 65 to 140 MeV

B. G. Ritchie, G. S. Blanpied, R. S. Moore, and B. M. Preedom
University of South Carolina, Columbia, South Carolina 29208

K. Gotow
Virginia Polytechnic Institute and State University, Blacksburg, Virginia 24061

R. C. Minehart, J. Boswell, and G. Das
University of Virginia, Charlottesville, Virginia 22901

H. J. Ziock
Los Alamos National Laboratory, Los Alamos, New Mexico 87545

N. S. Chant and P. G. Roos
University of Maryland, College Park, Maryland 20742

W. J. Burger, S. Gilad, and R. P. Redwine
Massachusetts Institute of Technology, Cambridge, Massachusetts 02139
(Received 22 November 1982)

Differential cross sections for the reaction $\pi^+ + d \rightarrow p + p$ were measured for pion laboratory energies of 65, 72.5, 80, 95, 110, 125, and 140 MeV. The integrated cross sections for these energies were found to be 7.51±0.19, 7.91±0.16, 8.64±0.15, 9.61±0.15, 11.3±0.2, 11.7±0.3, and 11.3±0.3 mb, respectively. These values indicate that the centroid and width of the energy dependence for the resonance in this reaction is lower and greater, respectively, than predicted by most theoretical models of the process. Comparisons made with predictions by Blankleider and Afnan show a qualitative difference between experimental measurements and calculations of the $P_4(\cos\theta)$ term in the polynomial expansion of the differential cross section. This may indicate a more important role for ρ-like exchange in the reaction mechanism than that included by the calculations.

[NUCLEAR REACTIONS $d(\pi^+,p)p$, $E=65$, 72.5, 80, 95, 110, 125, 140 MeV; measured absolute $d\sigma/d\Omega$, deduced total cross section; obtained fits to $P_n(\cos\theta)$ expansion; compared with Faddeev-type calculations for the reaction.]

INTRODUCTION

Pion absorption on the deuteron represents the simplest pion absorption process. A recent review[1] summarized the results of past measurements. Recently two experiments by Ritchie *et al.*[2] and Hoftiezer *et al.*[3] measured the total and differential cross sections for the reaction to high accuracy in the energy regions 20—65 and 113—140 MeV. These experiments, combined with earlier work below 20 MeV by Rose *et al.*[4] and above 140 MeV by Richard-Serre *et al.*,[5] have provided an important test for theories of the process. The results of these experiments define the energy dependence of the total cross section for the reaction quite well for $0 < E_\pi \leq 65$ MeV and $113 \leq E_\pi \leq 262$ MeV. The measurements also provided strong support for detailed balance for the $\pi^+ + d \leftrightarrows p + p$ reactions.

However, the region between 65 and 113 MeV possessed only sparse and imprecise data. The Hoftiezer data also seemed to suggest that the energy centroid and width of the peak in the total cross section was lower and wider, respectively, than suggested by then existing theoretical explanations of the process. The wide variations between the older and more recent measurements in the region below 140 MeV left a somewhat confused picture as to the trend of the total cross section and seemed to suggest structure within that energy range.

As the recent experiments have improved the

empirical description of the reaction process, the theoretical description has become more successful. A recent calculation by Blankleider and Afnan,[6] satisfying two and three body unitarity while coupling the $N-N$ and $\pi-d$ channels, has greatly improved the agreement between theory and experiment for the data below 140 MeV. The predictions of the theory for the observed angular distributions seemed to indicate that there was little necessity to include ρ exchange in those calculations to achieve agreement between theory and experiment. The predictions of a positive $P_4(\cos\theta)$ term up to 160 MeV in the parametrization of the differential cross section, however, did not agree with the Hoftiezer results. The region between 65 and 113 MeV was not sufficiently explored to permit accurate comparison between theory and experiment for the total and differential cross sections.

We report here measurements of the differential cross section for the reaction $\pi^+ + d \to p + p$ at seven energies between 65 and 140 MeV. The statistical accuracy obtained allowed determination of the total cross sections with an uncertainty of $<3\%$ for the energies studied. By overlapping the two previous studies by Ritchie *et al.* and Hoftiezer *et al.*, the description of the energy dependence of the total and differential cross sections is complete over the resonance in the $\pi^+ + d \to p + p$ reaction.

EXPERIMENTAL METHOD

The experiment was performed at the low energy pion (LEP) channel of the Clinton P. Anderson Meson Physics Facility. The channel was tuned to focus the pion beam into a spot smaller than 0.4 cm FWHM vertically and 1.1 cm FWHM horizontally. Beam spot size was determined using a multiwire profile monitor. The pion beam momentum spread was approximately 0.15% FWHM for 110, 125, and 140 MeV, and 0.25% FWHM for 65, 72.5, 80, and 95 MeV.

Pion decay monitors[7] were used for relative and absolute pion flux measurements. Each pion decay monitor detected the muons from the decay of pions in the incident beam and consisted of a pair of small plastic scintillators in coincidence. All monitors were positioned at an angle of less than 7° with respect to the beam, well within the Jacobian peak angle.

Absolute normalization of the pion decay monitors was accomplished in two steps.[8] Both steps were performed for each energy studied, with the LEP channel settings at each energy identical to those during the data taking runs, but with greatly reduced primary proton beam intensity. First, the number of particles per decay monitor count was determined using a pair of scintillators placed in the beam at the primary target position. A coincidence signal produced by a particle passing through the first scintillator into the second was fed into time-of-flight electronics with the LAMPF linac radio-frequency (rf) used as the "stop" signal. The time separation and relative intensities of the beam constituents were sufficient to permit determination of the number of particles per pion decay monitor event for each linac beam pulse. Average proton beam current during this portion of the experiment was several microamperes, or approximately two orders of magnitude less than beam intensity during normal data acquisition, to avoid saturating the in-beam scintillators. In the second step of this normalization procedure, the linac was operated so as to deliver one proton pulse to the pion production target every 40 nsec. The production target reaction products which were delivered to the scintillator pair within the LEP cave were very well separated by time of flight, since in this "chopped" mode the muons and electrons from later pulses of the linac did not overlap, as they did in the "unchopped" operation. In this manner, the pion fraction of the LEP beam could be determined to high precision (typically with an uncertainty of less than 0.5%) and, consequently, the number of pions per pion decay monitor event could be determined with considerable precision (an uncertainty of less than 1%). The validity of the normalization procedure was supported by the comparison of the results obtained here and previously published results[1,2,4] for the $\pi^+ + d \to p + p$ process at 65 and 140 MeV, and by $\pi^+ + p \to \pi^+ + p$ data taken during the experiment at each energy studied. (The results of the πp measurements will form the subject of an upcoming paper[9].)

A cryogenic liquid target filled with liquid deuterium was used as the primary target. The target was formed within a brass ring, using four parallel Mylar windows, and is shown schematically in Fig. 1. These windows formed three cells within the ring. The innermost pair of windows formed the liquid target cell, which held the cryogenic liquid target, while the outermost pair formed a gas pocket on either side of the liquid target cell. The gas pockets were filled by gas boiled off from the liquid cell and prevented the inner cell from bulging. The gas and liquid portions of the target formed a closed system. The target cell was 2.03 cm thick, the gas pockets were each 0.34 cm thick, and the diameter of the cell and gas pockets was 7.62 cm. An evacuated dummy target, identical to the primary target assembly, was mounted directly beneath the primary target and was used to determine all backgrounds from the liquid target. Both primary and dummy targets were mounted inside an insulating vacuum,

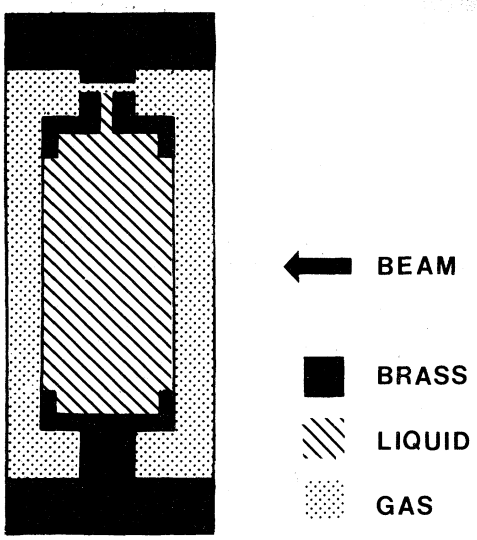

FIG. 1. A schematic sideview showing the basic design of the cryogenic target used in this experiment. Drawing is not to scale.

contained in a hollow aluminum cylinder approximately 32.5 cm in diameter, with Mylar windows. The total window thickness for target and vacuum chamber was 0.10 cm. The target bulging effects were negligible throughout the experiment. The pion beam struck the entrance window of the target at an angle of 30.3 deg.

The layout of the equipment in the LEP cave is shown schematically in Fig. 2. The detection system was a two-arm coincidence and time of flight measurement system which required a coincidence between a valid signal from one arm (E) (which measured the backward-going proton total energy) and the other arm (T) (which provided dE/dx information as the forward-going proton passed through it). The ten E detector systems consisted of NaI detectors thick enough to stop protons with kinetic energies up to 200 MeV, and small plastic scintillators (dE/dx disks) centered in front of the NaI detectors. The detector systems were spaced every 8° at a laboratory scattering angle from 93° to 165°, and remained fixed throughout the experiment. The dE/dx disks were of two sizes (nominally 3.8 and 1.9 cm in diameter), with the smaller size disks mounted on the three NaI detectors closest to the pion beam. All dE/dx disks were 65.7 ± 0.2 cm from the target center. The plastic scintillators provided dE/dx information on particles passing through them and, in coincidence with a valid signal from their respective NaI detectors, were used to generate an event signal for the E arm electronics. An E event coupled with a valid signal in the T arm (described next) yielded a "master event" signal, which served as a "start" signal for the time-of-flight (TOF) electronics.

The T arm consisted of two planes of plastic scintillator paddles. The front plane consisted of 15 overlapping paddles, 22.9 cm tall, 15.2 cm wide, and

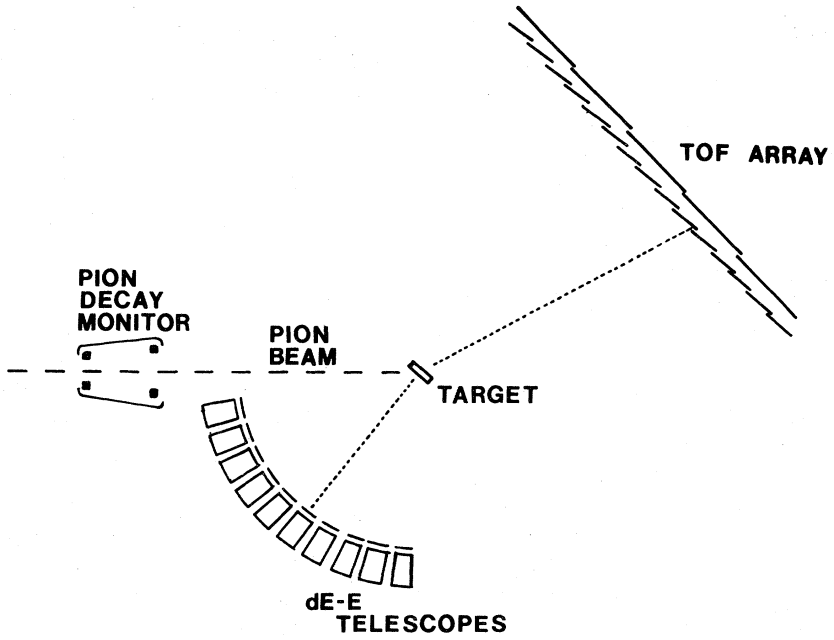

FIG. 2. Layout of apparatus used in this experiment. Drawing is not to scale.

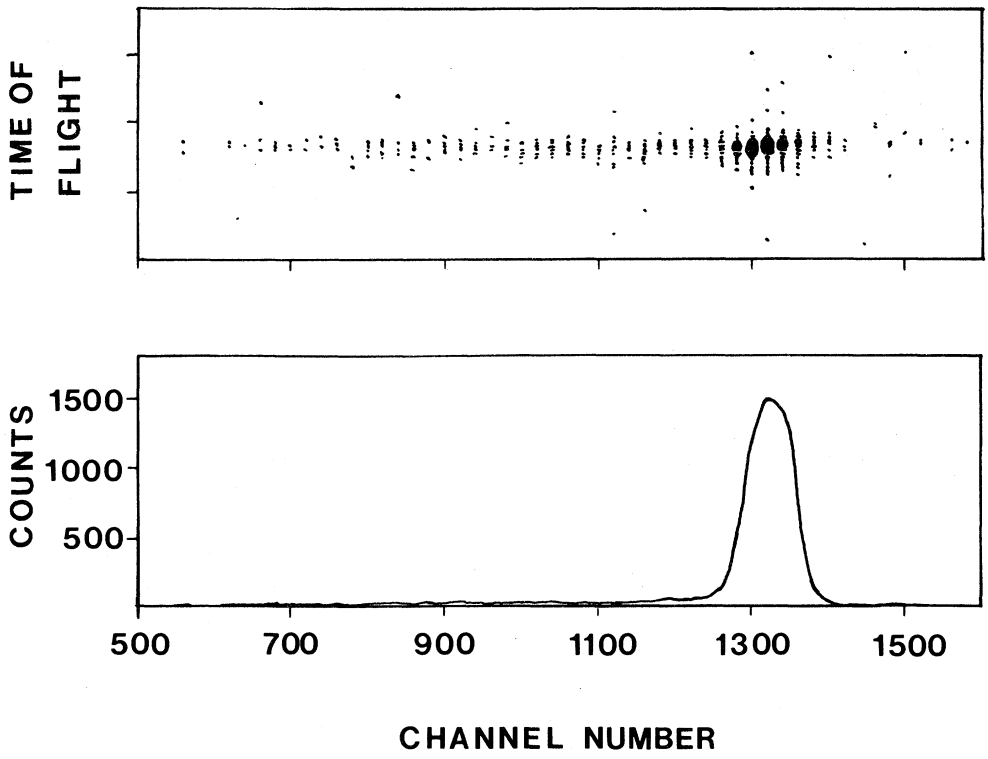

FIG. 3. Pulse height versus time of flight for a single detector system (upper figure) and the resultant pulse height spectrum (lower figure). Cuts have been made as described in that text. Reaction proton incident on the NaI in this case is 81 MeV.

0.64 cm thick. The back plane was formed by five overlapping paddles 25.4 cm tall, 50.8 cm wide, and with a thickness of either 0.64 or 0.95 cm. As indicated schematically in Fig. 2, the TOF planes were at an angle of 45° with respect to the beam, and were positioned such that the TOF paddles nearest the beam were 2 m downstream from the target. Signals generated by a particle passing through both layers were used to generate both a "stop" signal for the time-of-flight electronics and an event signal (when in coincidence with a valid signal in the E arm).

The logic pulse widths from the E and T arm counter electronics were adjusted so that the exact "start" and "stop" signals would occur with the dE/dx and front-paddle counter discrimination signals, respectively. This permitted a system time resolution of approximately 1 nsec, which was sufficient for resolving $\pi^+ + d \rightarrow p + p$ events from any background source, such as pion absorption on the nuclei within the Mylar windows. Additionally, accidental background from the target components was determined by taking data at each energy with the dummy target and subtracting the accidental background spectra, normalized by decay monitor events, from the foreground spectra.

Data were taken in two or more passes at each energy, except for one pass at 72.5 MeV. All detectors remained fixed in position throughout the data taking runs. All events were analyzed off line with cuts made on the events to restrict "good" events to those which possessed appropriate energy and kinematics for the reaction studied. An additional requirement demanded that good NaI events had E and dE values characteristic of reaction product protons. The resultant NaI spectra from the off-line analysis were clean and showed a spectrum typical of a monoenergetic proton beam stopped in NaI. These good events were correlated closely in time with the complimentary signals in the time-of-flight array. An example of this time correlation and the resultant energy spectra is shown in Fig. 3. Corrections were empirically measured and applied to correct for events lost by cutting across the tail of the NaI spectra. In general, statistical uncertainty at each angle measured was less than 1%. Electronics dead

TABLE I. Center of mass differential cross sections determined in this work for the reaction $\pi^+ + d \rightarrow p + p$. Errors listed for $d\sigma/d\Omega$ do not include absolute normalization uncertainty.

Incident pion energy (MeV)	Center of mass angle (deg)	$\frac{d\sigma}{d\Omega}$ (mb)	Error (mb)	Incident pion energy (MeV)	Center of mass angle (deg)	$\frac{d\sigma}{d\Omega}$ (mb)	Error (mb)
65.0	167.5	2.414	0.036		134.3	1.941	0.023
	160.7	2.234	0.034		127.1	1.612	0.018
	153.9	2.068	0.033		119.7	1.291	0.016
	147.0	1.969	0.024		112.2	1.056	0.014
	140.0	1.696	0.020		104.4	0.853	0.013
	132.9	1.500	0.019				
	125.6	1.203	0.015	110.0	168.3	3.746	0.060
	118.1	0.959	0.013		161.7	3.684	0.063
	110.5	0.774	0.011		155.1	3.055	0.042
	102.7	0.640	0.009		148.5	3.033	0.035
					141.8	2.565	0.029
72.5	167.6	2.588	0.041		134.8	2.311	0.026
	160.9	2.415	0.040		127.7	1.927	0.022
	154.2	2.208	0.037		120.4	1.533	0.019
	147.3	2.035	0.025		112.9	1.283	0.017
	140.4	1.784	0.023		105.1	1.024	0.014
	133.3	1.547	0.025				
	126.0	1.272	0.016	125.0	168.2	3.772	0.056
	118.6	1.025	0.014		162.3	3.552	0.055
	111.0	0.828	0.013		155.5	3.377	0.057
	103.1	0.707	0.020		148.9	3.106	0.038
					142.2	2.665	0.032
80.0	167.7	2.913	0.050		135.4	2.433	0.029
	161.1	2.712	0.036		128.3	2.115	0.026
	154.4	2.463	0.035		121.5	1.630	0.022
	147.6	2.252	0.026		113.6	1.357	0.019
	140.7	1.936	0.021		105.8	1.073	0.016
	133.6	1.709	0.020				
	126.4	1.414	0.016	140.0	162.1	3.321	0.096
	119.0	1.121	0.014		155.8	3.278	0.070
	111.4	0.916	0.012		149.3	2.988	0.039
	103.6	0.735	0.010		142.2	2.701	0.036
95.0	168.3	3.063	0.038		135.9	2.370	0.059
	161.4	2.988	0.038		128.9	2.027	0.034
	154.8	2.725	0.037		121.6	1.663	0.032
	148.1	2.529	0.029		114.2	1.375	0.021
	141.2	2.187	0.025		106.5	1.070	0.039

time for the detection system during data acquisition was negligible.

EXPERIMENTAL RESULTS

The differential cross section at each angle was determined from the relation

$$\left.\frac{d\sigma}{d\Omega}\right|_{\text{c.m.}} = \frac{N_p}{N_\pi}\frac{\cos\gamma}{\bar{n}\,d\Omega_{\text{lab}}}\frac{1}{J(E,\theta)}, \quad (1)$$

where for each energy E and laboratory angle θ, N_p represents proton pairs detected, with cuts and corrections applied as described above; N_π represents the number of pions incident on the target (determined from the decay monitor events as described above); γ represents the angle of the target relative to the beam ($30.3° \pm 0.3°$); $\bar{n}$ represents the target density ($9.94 \pm 0.10 \times 10^{22}$ deuterons/cm^2); $d\Omega$ represents the measured detection system solid angle at that angle; and $J(E\theta)$, represents the laboratory to center-of-mass Jacobian. The differential cross

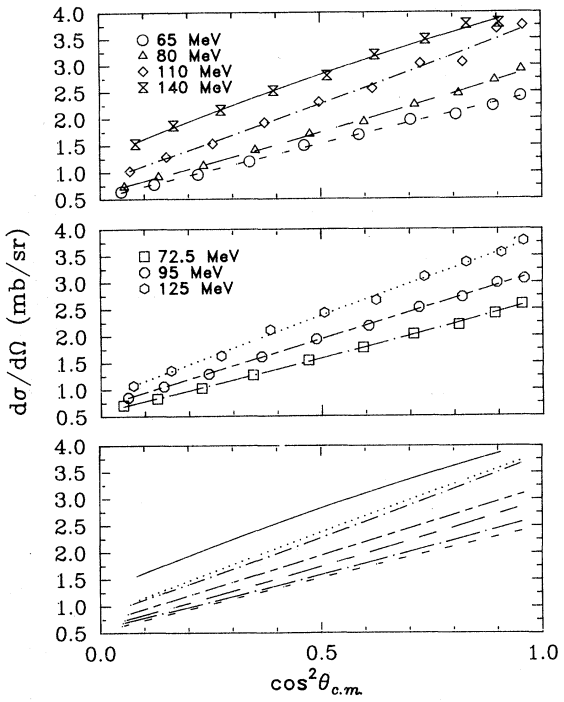

FIG. 4. Differential cross sections measured in this work, listed in Table I, and fits determined using Eq. (2) ($n=2$). Error bars do not exceed the size of the symbols. The lowest figure shows only the fitted curves to illustrate the energy dependence. Energies are pion laboratory kinetic energies. For clarity, 0.5 mb has been added to the 140 MeV data in these figures.

sections thus obtained are given in Table I and shown in Fig. 4.

The differential cross sections determined using Eq. (1) were fit to the phenomenological form

$$\left.\frac{d\sigma}{d\Omega}\right|_{\text{c.m.}} = \frac{1}{2\pi}\sum_{m=0}^{n}\alpha_{2m}P_{2m}(\cos\theta). \tag{2}$$

The values obtained from fits to this form with $n=1$ and $n=2$ are given in Table II. It should be noted from Table II that little statistically significant improvement was obtained by adding the $P_4(\cos\theta)$ term, except for the 140 MeV data. The fits with $n=2$ are also shown in Fig. 4.

Using this form, the total cross section is given by α_0. The results are plotted in Fig. 5 along with the data of Ritchie *et al.*,[2] Axen *et al.*,[10] Hoftiezer *et al.*,[3] and Richard-Serre *et al.*[5] The smooth trend of the total cross section energy dependence is evident. The centroid of the peak in the total cross section appears at approximately 130±10 MeV, somewhat lower than suggested by the older measurements not shown in Fig. 5.

The results obtained confirm the 65 MeV measurement of Ref. 2, and generally support the measurements of Ref. 3. The measurements of Stadler[11] are not supported by our results and, based on the smooth trend which we find for the energy dependence of the total cross section, must be in error. With Refs. 2, 3, and 5, and the results of this work, a complete set of high accuracy data now exists for the total and differential cross sections from 20 to 262 MeV.

TABLE II. Results of least squares fits to measured differential cross sections using Eq. (2). The parameters are given in units of mb/sr, with uncertainties enclosed in parentheses. Errors cited for the angular distribution parameters do not include normalization errors. Errors given for the total cross sections ($\Delta\sigma$) are absolute, including normalization and statistical error, and are given in mb.

	$n=1$				$n=2$				
E_π (MeV)	α_0	α_2	$\frac{X^2}{N_D}$	$\Delta\sigma$	α_0	α_2	α_4	$\frac{X^2}{N_D}$	$\Delta\sigma$
65	7.51	8.24	2.4	0.19	7.50	8.22	−0.21	2.6	0.19
	(0.05)	(0.13)			(0.05)	(0.14)	(0.19)		
72.5	7.88	8.64	0.9	0.16	7.91	8.61	0.24	0.7	0.16
	(0.04)	(0.10)			(0.04)	(0.09)	(0.14)		
80	8.61	9.67	1.9	0.13	8.64	9.70	0.31	1.4	0.15
	(0.05)	(0.13)			(0.08)	(0.22)	(0.29)		
95	9.61	10.50	0.9	0.15	9.61	10.50	0.00	1.0	0.15
	(0.04)	(0.10)			(0.04)	(0.10)	(0.14)		
110	11.31	12.30	6.5	0.23	11.33	12.31	0.27	7.1	0.25
	(0.08)	(0.33)			(0.13)	(0.34)	(0.64)		
125	11.74	12.70	3.8	0.30	11.72	12.71	−0.21	4.2	0.30
	(0.10)	(0.27)			(0.11)	(0.29)	(0.40)		
140	11.41	12.10	3.3	0.24	11.28	12.07	−0.86	2.1	0.26
	(0.04)	(0.38)			(0.11)	(0.26)	(0.39)		

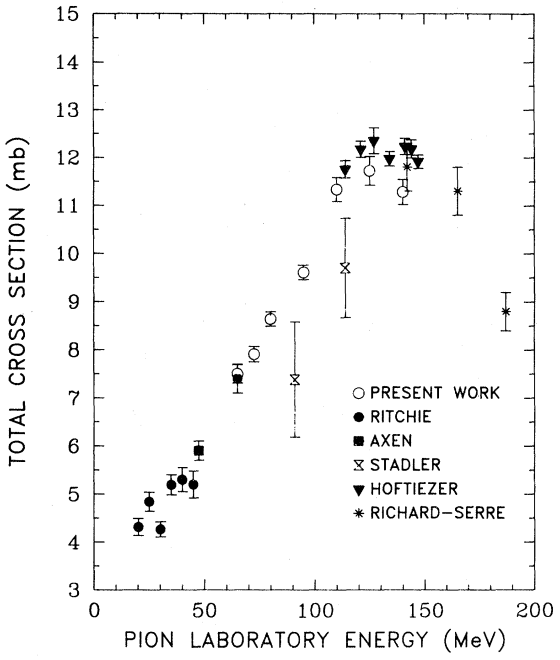

FIG. 5. Energy dependence of the total cross section for the reaction $\pi^+ + d \rightarrow p + p$.

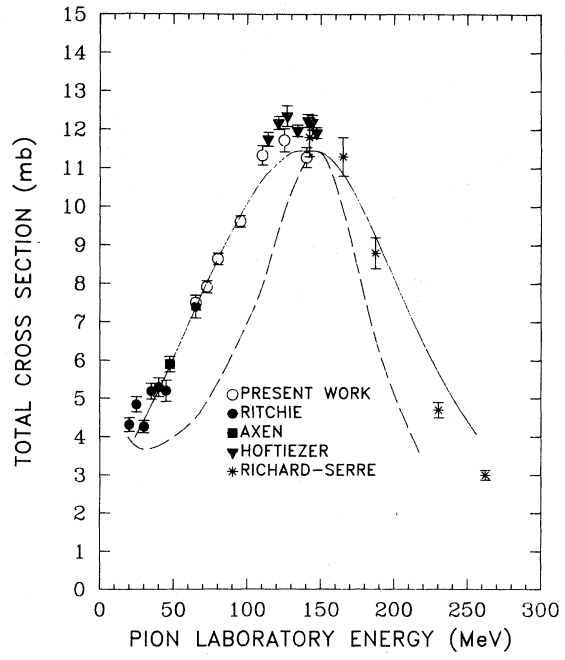

FIG. 6. Comparison of total cross section measurements and calculations by Blankleider and Afnan (Ref. 6) (solid curve) and by Niskanen (Ref. 12) (broken curve).

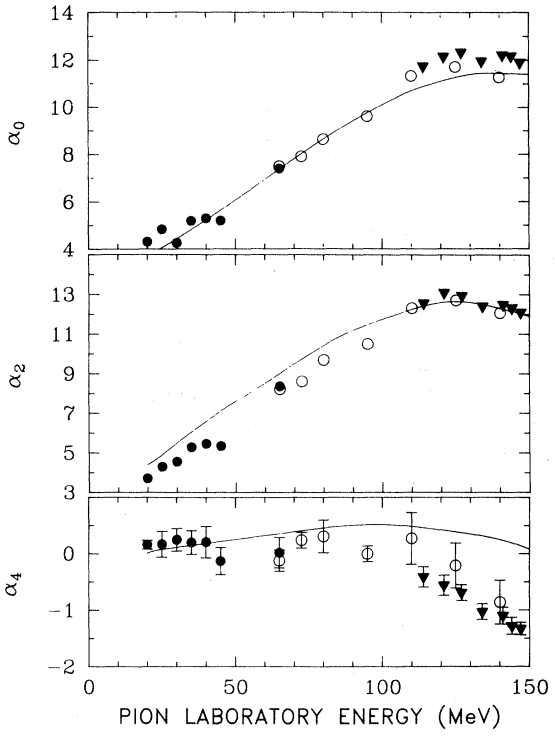

FIG. 7. Comparison of experimental values for the parameters of Eq. (2) with the predictions of Ref. 6. Symbols shown are as in Fig. 6.

DISCUSSION

Recently calculations for the $\pi^+ + d \rightarrow p + p$ reaction by Blankleider and Afnan[6] (BA) produced good quantitative agreement between experiment and theory for the total cross section energy dependence at low and resonance energies. As noted elsewhere,[2] previous calculations generally failed to reproduce the magnitude of either the observed low energy or resonance region total cross section.

The total cross sections measured here are shown with the BA calculation in Fig. 6, along with the experimental results of Refs. 2, 3, 5, and 10. The BA calculation does quite well, and the improvement over previous calculations is suggested by a comparison with the Niskanen[12] calculation, also shown in Fig. 6.

An additional test which must be applied to theories of the pionic disintegration of the deuteron is comparison with the experimentally observed differential cross sections. The results of this experiment [with $n=2$ in Eq. (2)] are shown in Fig. 7 compared with the BA predictions, along with the results of Refs. 2 and 3. It should be noted that for the data in Ref. 2 no statistically significant improvement in the fits to the observed differential

cross sections were obtained by adding a P_4 term to the fitting polynomial. The differential cross section results of Boswell *et al.*[13] also indicated that no such term was necessary at 80 MeV. Thus, though the results of Ref. 2 for α_4 are in accord with the BA predictions, caution must be exercised in interpreting the agreement as confirmation of the positive α_4 term predicted by BA. Indeed the BA calculation is perhaps unique in making such a prediction.

Regardless of any agreement below 60 MeV, the measurements here and in Ref. 2 do not support such a small positive term at 65 MeV and above. The general trend of the data indicates a smooth variation of α_4 near zero below 65 MeV to approximately -1.5 at 150 MeV. Consequently, the BA results are qualitatively different from the data, in particular concerning the energy at which α_4 for BA becomes negative. This discrepancy may arise from a greater contribution from ρ exchange than included in the calculation as noted by BA. Both Chai and Riska[14] and BA note that inclusion of ρ exchange generally contributes a negative $\cos^4\theta$ dependence which would alter the α_4 prediction. The BA approach, which produces a set of coupled Faddeev-type equations, implicitly includes some contribution from $T=1$ rescattering in the πNN form factor. Some of the strength of this rescattering term (particularly the crossed $\pi-\pi$ and $\rho-\rho$ diagrams) is not easily expressed in a Faddeev-type formalism due to the four-body nature of such a contribution. It is possible, therefore, that the inclusion of additional strength in the $T=1$ (ρ exchange) process would force α_4 to negative values more in agreement with experiment. The change in α_0 (and, thereby, the total cross section) would most probably be slight; inclusion of additional $T=1$ rescattering would probably move the predicted centroid of the total cross section predictions down somewhat and marginally improve agreement with experiment.

CONCLUSIONS

The results of this work have established the smooth trend of the total cross section energy dependence from 65 to 140 MeV. The angular distribution parameters also have been shown to vary smoothly, though the trend for α_4 is somewhat uncertain. The recent calculations of Blankleider and Afnan have been shown to agree reasonably well with experiment, with the exception of the α_4 parameter prediction. The α_4 empirical energy dependence appears to be qualitatively different from the BA prediction and may indicate the importance of ρ exchange in the reaction mechanism.

ACKNOWLEDGMENTS

The authors wish to thank the following: R. L. Burman and M. V. Hynes of Los Alamos National Laboratory for their assistance and discussions in the planning and execution of this experiment; Fred Myhrer for helpful discussions of theoretical aspects of the process; Boris Blankleider for providing copies of the results of the BA calculations; the administration at LAMPF for providing low intensity beam time for the normalization runs; the LAMPF operation and experiment support staffs, particularly Gil Suazo, Jan Novak, Larry Marek, and O. B. Van Dyck, for their valuable assistance in the design and execution of this experiment; and F. E. Bertrand for the use of several NaI detectors. We also wish to thank the following for their assistance during the data taking portion of this work: M. Artuso and C. Magno (V.P.I. and S.U.); C. Mishra (U.S.C.); G. Ciangaru, L. Rees, and J. Wesick (U.Md.); and R. Marshall (U.Va.). This work was supported in part by the National Science Foundation and by the Department of Energy.

[1]G. Jones, in *Pion Production and Absorption in Nuclei—1981 (Indiana University Cyclotron Facility)*, Proceedings of the Conference on Pion Production and Absorption in Nuclei, AIP Conf. Proc. No. 79, edited by Robert D. Bent (AIP, New York, 1982).

[2]B. G. Ritchie *et al.*, Phys. Rev. C 24, 552 (1981).

[3]J. Hoftiezer *et al.*, Phys. Lett. 100B, 462 (1981); and (private communication).

[4]C. M. Rose, Phys. Rev. 154, 1305 (1967).

[5]C. Richard-Serre *et al.*, Nucl. Phys. B20, 413 (1970).

[6]B. Blankleider and I. R. Afnan, Phys. Rev. C 24, 1572 (1981).

[7]E. A. Wadlinger, Nucl. Instrum. Methods 134, 243 (1976).

[8]M. D. Cooper, Los Alamos Scientific Laboratory Report LA-55-29-MS, 1974.

[9]B. G. Ritchie *et al.*, Phys. Lett. B (to be published).

[10]D. Axen *et al.*, Nucl. Phys. A256, 387 (1976).

[11]H. L. Stadler, Phys. Rev. 96, 496 (1954).

[12]J. A. Niskanen, Nucl. Phys. A298, 417 (1978).

[13]J. Boswell *et al.*, Phys. Rev. C 25, 2540 (1982).

[14]J. Chai and D. O. Riska, Nucl. Phys. A338, 349 (1980).